Available online at www.sciencedirect.com
ScienceDirect
Journal of Molecular Graphics and Modelling 26 (2008) 1269–1275
Journal of Molecular Graphics and Modelling
www.elsevier.com/locate/JMGM

Thermodynamic and mechanical properties of epoxy resin DGEBF crosslinked with DETDA by molecular dynamics

Jeremy L. Tack [a,1], David M. Ford [b,*]

[a] Department of Chemical Engineering, Texas A&M University, College Station, TX 77843-3122, USA
[b] Department of Chemical Engineering, University of Massachusetts-Amherst, Amherst, MA 01003, USA

Received 14 August 2007; received in revised form 29 November 2007; accepted 2 December 2007
Available online 28 January 2008

Abstract

Fully atomistic molecular dynamics (MD) simulations were used to predict the properties of diglycidyl ether of bisphenol F (DGEBF) crosslinked with curing agent diethyltoluenediamine (DETDA). This polymer is a commercially important epoxy resin and a candidate for applications in nanocomposites. The calculated properties were density and bulk modulus (at near-ambient pressure and temperature) and glass transition temperature (at near-ambient pressure). The molecular topology, degree of curing, and MD force-field were investigated as variables. The models were created by densely packing pre-constructed oligomers of different composition and connectivity into a periodic simulation box. For high degrees of curing (greater than 90%), the density was found to be insensitive to the molecular topology and precise value of degree of curing. Of the two force-fields that were investigated, cff91 and COMPASS, the latter clearly gave more accurate values for the density as compared to experiment. In fact, the density predicted by COMPASS was within 6% of reported experimental values for the highly crosslinked polymer. The predictions of both force-fields for glass transition temperature were within the range of reported experimental values, with the predictions of cff91 being more consistent with a highly cured resin.

Keywords: Epoxy; Crosslinked polymer; Molecular dynamics; Modulus; Glass transition

1. Introduction

In this section we describe the rationale for this study, previous molecular modeling work in related areas, and the specific objectives of this work.

1.1. Background

Currently there is significant research and development activity in nanocomposites based on epoxy resin matrices [1–3]. The inclusion of nanometer-scale inorganic materials at small weight fraction can yield tremendous enhancements in thermophysical properties of a cured epoxy. Choices of nanofiller range from natural clays [4] to synthetic metal oxides [5] to carbon nanotubes [6]. One specific example of a system of interest is carbon nanotubes dispersed in epoxy EPON^{TM} 862 [7], or diglycidyl ether of bisphenol F (DGEBF) crosslinked by diethyltoluenediamine (DETDA) [8–10]. However, creating nanocomposites with enhanced properties has proven challenging, especially with respect to achieving good dispersion of the nanofiller. Molecular modeling has been proposed as a tool to advance the field.

1.2. Previous molecular modeling work

Modeling the effects of nanometer-scale fillers on polymer matrices is challenging due to the breadth of relevant time and length scales [11]. One particular problem for epoxy matrices is that highly crosslinked networks present a unique set of challenges for molecular modeling, as discussed in the recent literature. Svaneborg et al. created crosslinked networks of freely jointed bead-spring chains by superimposing a stochastic linking procedure on a molecular dynamics (MD) trajectory, yielding disordered networks consistent with rubbery polymers [12]. Hamerton et al. created a model polycyanurate by constructing fundamental repeat units at the atomistic scale and chemically joining them in a three-dimensional superlattice,

* Corresponding author. Tel.: +1 413 577 0134; fax: +1 413 545 1647.
E-mail addresses: jtack13@yahoo.com (J.L. Tack), ford@ecs.umass.edu (D.M. Ford).
[1] Tel.: +1 979 862 1079; fax: +1 979 845 6446.

1093-3263/$ – see front matter © 2007 Elsevier Inc. All rights reserved.
doi:10.1016/j.jmgm.2007.12.001

yielding a quasi-crystalline representation [13]. Wu and Xu created a model epoxy using a proximity-based crosslink creation algorithm applied progressively throughout an MD trajectory, starting from a dense fluid of monomer and linker molecules [14]. We note that the atomistic modeling work of Wu and Xu [14] is on an epoxy that is quite similar to DGEBF–DETDA, namely diglycidyl ether of bisphenol A (DGEBA) crosslinked with isophorone diamine (IPD), and thus provides a point of comparison for the research reported here.

Previous molecular modeling literature on the specific system DGEBF–DETDA is very limited. Gou et al. [10] carried out a combined computational and experimental study of DGEBF–DETDA interacting with single walled carbon nanotubes (SWNT). The computational work employed models of oligomeric epoxy species packed around one SWNT at a set density of 1.2 g/cc and temperature of 298 K. They calculated the interfacial bonding energy between the epoxy and the nanotube to be 0.1 kcal/(mol Å^2). Using pullout simulations they estimated an interfacial shear strength of 75 MPa. In the experimental study they found uniform dispersion and good interfacial bonding of the nanotubes in the epoxy resin, resulting in a 250–300% increase in the storage modulus with an addition of 20–30 wt.% nanotubes.

1.3. Objectives of this study

As a step in understanding nanocomposites based on DGEBF–DETDA resins, we have carried out atomistic modeling of neat polymers with an emphasis on predicting certain key thermodynamic and mechanical properties: density, bulk modulus, and glass transition temperature. This work will establish a baseline for future modeling of the same properties in nanocomposites. Molecular topology and degree of crosslinking are likely two critical parameters that determine the resin's effectiveness in staying bonded to carbon nanotubes under loading, and thus their effects on the bulk material properties are important to understand. Another major issue is determining which force-fields give the most accurate property predictions as compared to experimental data; here we have compared two commonly used force-fields, COMPASS and cff91. This atomistic modeling research will complement ongoing experimental studies of the DGEBF–DETDA system using traditional and nanoscale characterization techniques.

Section 2 of this paper describes how the atomistic models were built, how the MD simulations were performed, and how the properties of interest were calculated. The results are presented in Section 3 and the conclusions are discussed in Section 4.

2. Model and simulation details

2.1. Molecular structure in DGEBF–DETDA

Before building the atomistic models, it is instructive to consider how DGEBF and its DETDA-cured polymeric forms are synthesized. Fig. 1 shows the synthesis of a DGEBF monomer from bisphenol F and an epoxide; the R-group in the epoxide is typically chlorine. The reactant bisphenol F, and the product DGEBF monomer, may be in one of three different structural forms: *ortho–ortho*, *para–para*, or *para–ortho*; only the *para–para* form is shown in Fig. 1. During the synthesis a newly formed DGEBF monomer can also undergo a polyaddition reaction with bisphenol F as seen in Fig. 2, to form a polyether product; this reaction can be enhanced by temperature and an appropriate catalyst [15].

Next we consider the crosslinking of DGEBF monomer (or its extended polyether form) with DETDA. Fig. 3 shows the reaction of an epoxide group at the end of the DGEBF monomer with an amine group on the DETDA. Note that the resulting product may react with up to three more epoxide groups, since there are still three hydrogen atoms remaining between the two amine groups. Fig. 4 shows the start of such further crosslinking, which ultimately leads to the formation of a networked polymer.

In summary, when building the molecular models of crosslinked DGEBF–DETDA there are choices to be made regarding:

- *ortho*/*para* structural conformation of DGEBF monomers;
- fraction of polyether species present (Fig. 2);
- degree of crosslinking and molecular topology.

We consider each of these as a variable to be explored in our simulation study.

2.2. Building the atomistic models

We have followed the approach of Gou et al. [10] in using densely packed oligomeric molecules as an approximation to the fully networked polymer. More specifically, our procedure involved creating a set of about 10 crosslinked oligomers (in some cases diluted with unreacted DGEBF monomer and DETDA molecules) and densely packing them into a periodic box using standard algorithms. This is in contrast to the more complex network-building approaches cited above. Later we will compare and contrast our results with those of Wu and Xu [14], who have modeled a similar epoxy (DGEBA–IPD) using a

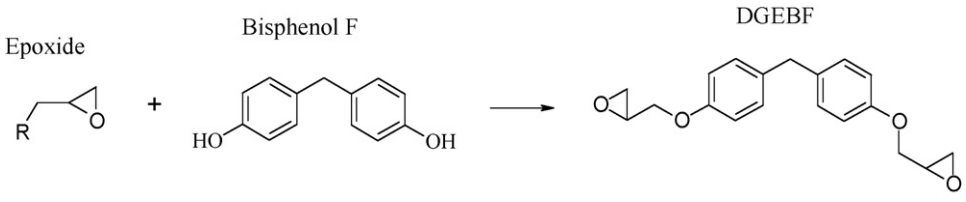

Fig. 1. Formation of a DGEBF monomer.

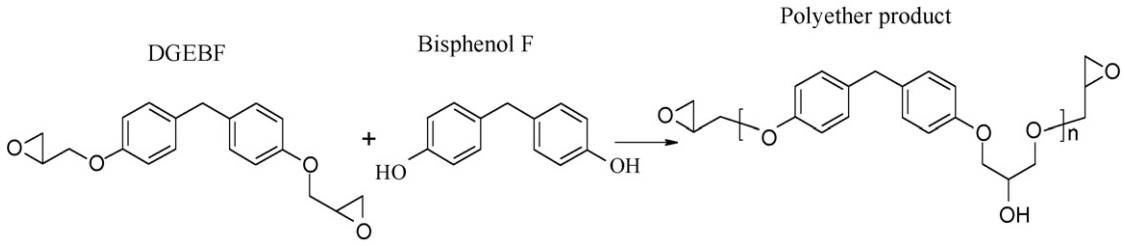

Fig. 2. Polyaddition of bisphenol F to DGEBF, forming a polyether product.

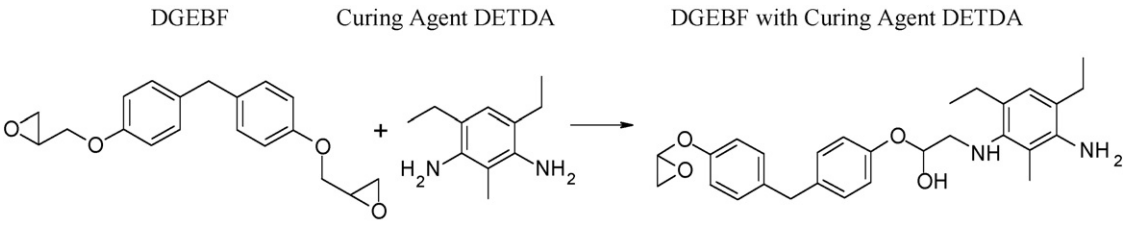

Fig. 3. Reaction of DGEBF monomer with curing agent DETDA.

different network-building approach. Next we describe the particular models built for this study.

2.2.1. *Oligomeric models based on normal monomers of DGEBF*

Product information from a manufacturer of DGEBF–DETDA resins states that the typical ratio of monomer to curing agent in the final resin is 100/26.4 by weight [16]. This implies a number ratio of 2.15 normal DGEBF monomers to one DETDA molecule. Within that constraint we built two different types of oligomer model, which we call "square oligomer" and "triangle oligomer"; they are shown in Figs. 5 and 6, respectively. Each oligomer was built from 13 DGEBF monomers and six DETDA molecules, but they clearly have different topologies. These oligomeric models, and others described below, were created in the Materials Visualizer environment within the Materials Studio software product from Accelrys Inc. [17].

2.2.2. *Oligomeric models based on the polyether product of DGEBF*

We also built model oligomers that included the polyether product of DGEBF, as shown in Fig. 2, with $n = 2$. More

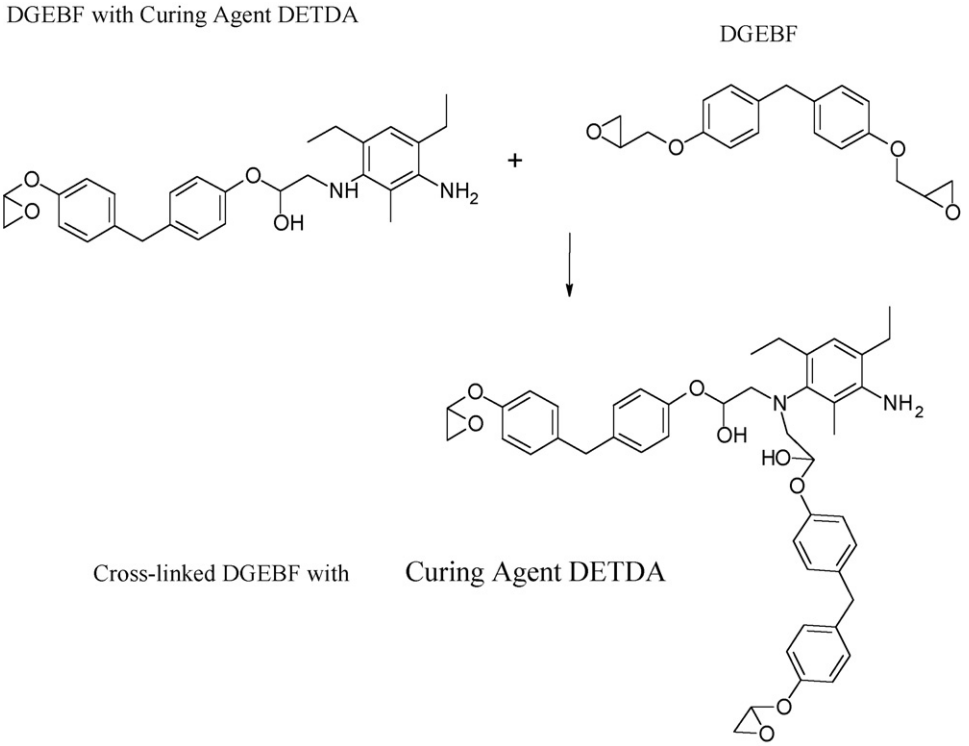

Fig. 4. Start of the crosslinking process to form DGEBF–DETDA resin.

Fig. 5. A ‘‘square’’ oligomer of DGEBF crosslinked by DETDA.

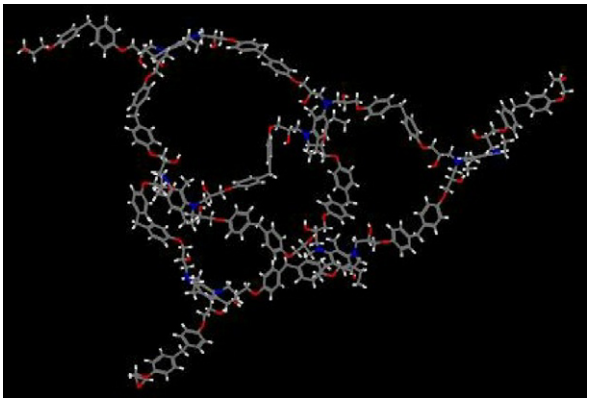

Fig. 6. A ‘‘triangular’’ oligomer of DGEBF crosslinked by DETDA.

specifically, we built oligomers composed of one $n = 2$ polyether, seven normal DGEBF monomers, and four DETDA molecules in a square configuration, which is basically a smaller version of the topology pictured in Fig. 5. We will refer to this molecule as the ‘‘polyether oligomer’’. The polyether oligomer also satisfies the target weight ratio of 100/26.4. Finally, we explored the role of structural isomers by constructing some polyether oligomers using exclusively the *ortho–ortho* conformation of its DGEBF constituents, and others using exclusively the *para–para* conformation.

2.2.3. Preparing dense amorphous models for simulation

We created atomistic models of different amorphous systems by selecting the desired number and type of oligomer molecules (and any other constituents) and then stochastically packing them into a periodic simulation volume.

We first built sets of models based on the square and triangle oligomers shown in Figs. 5 and 6. The ‘‘square model’’ was composed of 10 square oligomers, and the ‘‘triangle model’’ was composed of 10 triangle oligomers. These models can be considered representative of completely cured resins, because every DGEBF monomer is linked to at least one other DGEBF monomer through a DETDA crosslinker (the accuracy of the network topology is a separate issue). We also built a model to represent a resin that is only partially cured, at a level of approximately 90%. This model, called ‘‘cured90’’, comprised nine square oligomers plus 13 unbonded DGEBF monomers and six unbonded DETDA molecules. Finally, as an interesting limiting case, we constructed a completely uncured model called ‘‘liquid’’, which consisted solely of unbonded DGEBF monomers and DETDA molecules.

We also built models that included the polyether oligomer and different structural isomers, as described in the previous section. The ‘‘*ortho–ortho* model’’ was composed of 10 polyether oligomers (described in Section 2.2.2) with all DGEBF units in the *ortho–ortho* conformation. The ‘‘*para–para* model’’ was composed of 10 polyether oligomers with all DGEBF units in the *para–para* conformation (as in Fig. 1). These two models can be considered representative of completely cured resins. We also built a ‘‘partly cured model’’ comprising nine polyether oligomers, seven unbonded DGEBF monomers, one unbonded polyether product molecule (i.e. the product in Fig. 2), and four unbonded DETDA molecules; all DGEBF units were in the *para–para* configuration for the ‘‘partly cured’’ model.

For each model we used the Amorphous Cell module in Materials Studio to create the dense periodic packing. Amorphous Cell was used to place the selected molecules into a periodic cell initially at a density lower than the target density. The periodic cell length parameters were then decreased in small increments, with local energy minimization carried out after each change, until the target density was reached. The building process was followed by short (20 ps) trajectories of canonical and isothermal–isobaric molecular dynamics to stabilize the temperature and pressure near 298 K and 1 atm before further dynamics runs. This building process was repeated multiple times for a given system, to provide (1) a sampling of different starting points for the dynamics and (2) a basis for estimating uncertainties on the calculated properties.

Fig. 7 shows two views of a square model packed into a periodic box. Since the individual oligomers (Fig. 5) are somewhat two-dimensional by construction, one concern is that the final packed models might have unrealistic structural anisotropies (although the techniques of Amorphous Cell are designed to avoid this situation). From visual inspection of the packed models, using representations like Fig. 7 and also the free-volume tool in Materials Visualizer, there were no obvious indications of anisotropic conditions.

2.3. Running the molecular dynamics

Two different simulation programs were used to generate the molecular dynamics (MD) trajectories on the models. One was LAMMPS, a freely available code developed by Plimpton at Sandia National Laboratories [18,19]. LAMMPS has the advantages of being open source and intrinsically designed for parallel implementation, but it is currently limited to the use of an orthorhombic simulation box. The other MD program used in this study was Discover, which is another module within Materials Studio. Discover has several advantages, including access to the proprietary COMPASS force-field, support for non-orthorhombic simulation boxes, and simplicity in importing the molecular model. (A translator program was

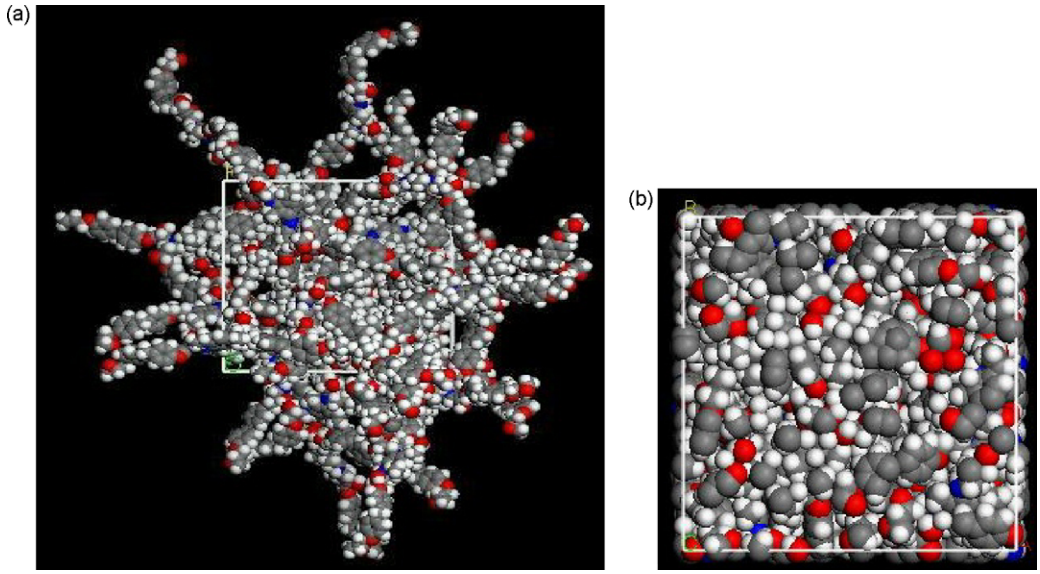

Fig. 7. Two views of the square model system densely packed into a periodic box. View (a) is the default view where chemically bonded species are represented in extended form, while view (b) implements the coordinate wrapping procedure consistent with periodic boundary conditions.

needed to import the models into LAMMPS from the Materials Studio environment.) However, we discovered some limitations in model size and job speed while running the Materials Studio software on our single-processor PC, as compared to running LAMMPS on an Apple G5 cluster. These limitations forced us to reduce the number of molecules employed in the simulations by a factor of two (based on the numbers given in Section 2.2.3) when running MD with Discover. In summary, we used LAMMPS as the main workhorse but changed to Discover when evaluating the proprietary COMPASS force-field. The cff91 force-field, which is freely available and transferable to any MD simulation software, was the other option evaluated in this study.

We generally employed the isothermal–isobaric, or *NpT*, ensemble. Within LAMMPS we used the Nose-Hoover method for both temperature and pressure control. Within Discover we used the Berendsen method for both temperature and pressure control. For both programs the Ewald summation was used to calculate the long-range Coulombic forces. Each model was initially run for 100–500 ps, until equilibrium or steady-state behavior was observed, and then run for 100–1000 ps to evaluate the desired properties.

2.4. Property predictions

2.4.1. Density

The density was simply obtained from an *NpT* simulation by dividing the total mass of atoms in the simulation cell by the average cell volume over the MD production run.

2.4.2. Bulk modulus

The bulk modulus can be simply determined by estimating the volume change induced by a specified change in hydrostatic pressure and applying the following equation:

$$B = \frac{\Delta p}{(\Delta V / V_0)} \tag{1}$$

In practice we used 1 atm as the base state and 5000 atm as the new state when evaluating B via Eq. (1); the volumes were simply the average simulation box volumes determined at equilibrium under the two different pressure conditions. The temperature was maintained at 298 K.

2.4.3. Glass transition temperature

We evaluated equilibrium density across a range of temperatures at $p = 1$ atm using molecular simulation; the glass transition temperature T_g is identified as the temperature at which the density *vs.* temperature data showed a discontinuous change in slope [20].

3. Results

3.1. Effects of topology and degree of curing on density

Table 1 summarizes the density predictions from the oligomeric models based on normal monomers of DGEBF (described in detail in Sections 2.2.1 and 2.2.3). All runs were performed with LAMMPS using the cff91 force-field at 298 K and 1 atm. These four models show that the molecular topology and degree of curing (above 90%) does not have a statistically significant effect on the density. On the other hand, the completely unbonded (liquid) model does predict a density significantly lower than all of the oligomer-based models. As a point of experimental comparison, a manufacturer of DGEBF–DETDA resins reports a density of 1.20 g/cc based on a cure schedule of 1.5 h at 350 °F [16]. All of the models in Table 1 underpredict this experimental value by about 10–15%.

Table 1
Comparison of predicted density for different models

	cured90	Liquid	Square	Triangle
Average density (g/cc)	1.067	1.011	1.054	1.039
Range	1.061–1.078	1.002–1.024	1.036–1.061	1.018–1.049
Standard deviation	0.0088	0.0085	0.012	0.014
MD time per replicate (ps)	600	1000	600	900
Number of replicates	5	5	4	4

Table 2 summarizes the data for the models that included a polyether form of DGEBF and also explored structural isomerism within the monomer unit (described in detail in Sections 2.2.2 and 2.2.3). All runs were performed with LAMMPS using the cff91 force-field at 298 K and 1 atm. The predicted densities were not significantly different from those reported for the different oligomeric models in Table 1.

Our main conclusion from this part of the work was that the molecular topology of the oligomers does not have a significant effect on density, unless one approaches the limit of liquid-like dissociated monomers. The ''square model'' based on normal DGEBF monomer will therefore be used for the rest of the work.

3.2. Effects of force-field on density

Next we explored the effects of force-field on the predicted density. MD trajectories using COMPASS were performed with Discover, and trajectories using cff91 were performed with LAMMPS. All runs were at 298 K and 1 atm using the ''square model'' with a reduced number of oligomer molecules, as described in Section 2.3. The results in Table 3 show that the COMPASS force-field predicted a significantly higher density than the cff91. The effect of the force-field choice on predicted density was surprisingly much more substantial than the effect of the specific oligomeric model employed. The density predicted by the COMPASS force-field is about 6% lower than the experimental value of 1.20 g/cc, as compared to 11% lower with cff91.

3.3. Bulk modulus

Runs using COMPASS were performed with Discover, and runs using cff91 were performed with LAMMPS. All runs were at 298K using the ''square model'' with a reduced number of oligomer molecules, as described in Section 2.3. The values of the bulk modulus are summarized in Table 4. The modulus predicted by the cff91 force-field is greater than that predicted by the COMPASS force-field, although the predictions actually fall within each others' range of uncertainty as estimated across different initial starting configurations of the model. Perhaps the closest point of comparison for our data is the value $B = 5.804$ GPa reported by Wu and Xu [14] using the COMPASS force-field on a similar model epoxy (DGEBA–IPD). This is slightly higher than the value that we predict using COMPASS; without further study, we cannot say whether the discrepancy is due to the different chemical composition of the two epoxies or the different network-building technique employed. We note that the bulk moduli values from simulation are all significantly higher than the experimental value of $B = 5.01$ GPa cited for DGEBA–IPD [21]. Overprediction of bulk and shear moduli is common with molecular simulation, because the effects of macroscopic or even large microscopic defects are not included. The simulated values are therefore frequently regarded as an upper limit on the experimental values [22].

Table 2
Comparison of predicted density for different polyether-containing models

	ortho–ortho	*para–para*	Partly cured
Average density (g/cc)	1.073	1.075	1.07
Range	1.054–1.082	1.058–1.083	1.068–1.074
Standard deviation	0.0114	0.0105	0.0028
MD time per replicate (ps)	100	100	100
Number of replicates	5	5	3

3.4. Glass transition temperature

Fig. 8 is a plot of predicted density as a function of temperature for the two different force-fields. Runs using COMPASS were performed with Discover and runs using cff91 were performed with LAMMPS. All runs were at 298 K using the ''square model'' with a reduced number of oligomer molecules, as described in Section 2.3. Using the discontinuity in the slope to locate T_g, we found that COMPASS predicts a value between 350 and 400 K and cff91 predicts a value between 400 and 425 K. A manufacturer of DGEBF–DETDA resins reports experimental T_g on the range 386–434 K, depending on the curing temperature and schedule (with higher values corresponding to greater cure temperatures and times) [16]. On their face, these data do little to recommend one force-field over the other. However, if we assume our fully crosslinked models correspond to the more

Table 3
Comparison of density predicted by different force-fields

	cff91	COMPASS	Experimental
Average density (g/cc)	1.074	1.13	1.20
Range	1.054–1.082	1.123–1.1345	
Standard deviation	0.0104	0.0061	

Table 4
Prediction of bulk modulus

Bulk modulus B (GPa)	
cff91	5.79 ± 0.21
COMPASS	5.18 ± 0.54

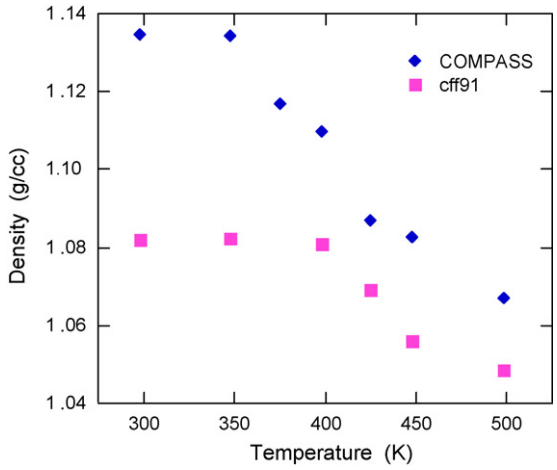

Fig. 8. Predicted density as a function of temperature at 1 atm for the "square model".

aggressive curing conditions, we would conclude that the cff91 force-field is the more accurate predictor of T_g.

4. Conclusions

This study of DGEBF with curing agent DETDA using MD simulation focused on three main points: predicting key thermodynamic and mechanical properties; evaluating the effects of molecular topology on the predictions; and determining which force-field gives the most realistic results as compared to experiment. For high degrees of cure, the molecular topology had remarkably little effect on the density predictions; only the completely unbonded (liquid) model showed large differences from the others. The density predictions were sensitive to the force-field used, with COMPASS giving the better result (which was 6% lower than the experimental value). Both COMPASS and cff91 predicted glass transition temperatures in the experimental range, with the cff91 result being higher. We do not have experimental bulk modulus data on DGEBF–DETDA with which to compare directly, but our calculated bulk moduli were consistent with simulation predictions in the literature for a similar epoxy.

Overall we conclude that the "assembled oligomer" approach to building crosslinked epoxy structure employed here (and previously by Guo et al. [10]) gives reasonably accurate predictions for basic thermodynamic and mechanical properties using currently available force-fields. Future work will focus on a direct comparison to different network-building techniques and the prediction of mechanical properties involving shear.

Acknowledgements

This research was funded by the United States Air Force Research Laboratory, Materials and Manufacturing Directorate, AFRL/MLBC, under the Air Force Minority Leaders Program, contract number FA8650-05-D-1912. The authors would like to thank Professors John D. Whitcomb and Tahir Cagin for their helpful advice during the course of this research.

References

[1] F. Hussain, M. Hojjati, M. Okamoto, R.E. Gorga, Review article: polymer-matrix nanocomposites, processing, manufacturing, and application: an overview, J. Compos. Mater. 40 (2006) 1511–1575.
[2] N. Karak, Polymer (epoxy) clay nanocomposites, J. Polym. Mater. 23 (2006) 1–20.
[3] K.K. Maniar, Polymeric nanocomposites: a review, Polym.-Plast. Technol. Eng. 43 (2004) 427–443.
[4] X.Y. Meng, Z. Wang, T. Tang, Controlling dispersed state and exfoliation process of clay in polymer matrix, Mater. Sci. Technol. 22 (2006) 780–786.
[5] J. Liu, W.J. Boo, A. Clearfield, H.J. Sue, Intercalation, exfoliation:, A review on morphology of polymer nanocomposites reinforced by inorganic layer structures, Mater. Manuf. Process. 21 (2006) 143–151.
[6] M. Moniruzzaman, K.I. Winey, Polymer nanocomposites containing carbon nanotubes, Macromolecules 39 (2006) 5194–5205.
[7] Hexion Specialty Chemicals, Product Bulletin EPON Resin 862. Available from: http://www.hexionchem.com/pds/E/EPON%20Resin%20862.pdf.
[8] S.R. Wang, Z.Y. Liang, T. Liu, B. Wang, C. Zhang, Effective amino-functionalization of carbon nanotubes for reinforcing epoxy polymer composites, Nanotechnology 17 (2006) 1551–1557.
[9] Z.Y. Liang, J.H. Gou, C. Zhang, B. Wang, L. Kramer, Investigation of molecular interactions between (10,10) single-walled nanotube and Epon 862 resin/DETDA curing agent molecules, Mater. Sci. Eng. A: Struct. Mater. Prop. Microstruct. Process. 365 (2004) 228–234.
[10] J.H. Gou, B. Minaie, B. Wang, Z.Y. Liang, C. Zhang, Computational and experimental study of interfacial bonding of single-walled nanotube reinforced composites, Comput. Mater. Sci. 31 (2004) 225–236.
[11] V.A. Buryachenko, A. Roy, K. Lafdi, K.L. Anderson, S. Chellapilla, Multi-scale mechanics of nanocomposites including interface: experimental and numerical investigation, Compos. Sci. Technol. 65 (2005) 2435–2465.
[12] C. Svaneborg, G.S. Grest, R. Everaers, Disorder effects on the strain response of model polymer networks, Polymer 46 (2005) 4283–4295.
[13] I. Hamerton, B.J. Howlin, P. Klewpatinond, H.J. Shortley, S. Takeda, Developing predictive models for polycyanurates through a comparative study of molecular simulation and empirical thermo-mechanical data, Polymer 47 (2006) 690–698.
[14] C.F. Wu, W.J. Xu, Atomistic molecular modelling of crosslinked epoxy resin, Polymer 47 (2006) 6004–6009.
[15] M. Kobayashi, F. Sanda, T. Endo, Application of phosphonium ylides to latent catalysts for polyaddition of bisphenol A diglycidyl ether with bisphenol A: model system of epoxy-novolac resin, Macromolecules 32 (1999) 4751–4756.
[16] Hexion Specialty Chemicals, Product Bulletin EPIKOTE Resin 862/ EPIKURE Curing Agent W System. Available from: http://www.hexionchem.com/pds/E/EPIKOTE(%20Resin%20862%20EPIKURE(%20Curing%20Agent%20W.pdf.
[17] Materials Studio, 2007, Accelrys, Inc. Available from: http://www.accelrys.com/products/mstudio/.
[18] LAMMPS WWW Site, 2007, Sandia National Laboratories. Available from: http://lammps.sandia.gov/.
[19] S. Plimpton, Fast parallel algorithms for short-range molecular-dynamics, J. Comput. Phys. 117 (1995) 1–19.
[20] J. Han, R.H. Gee, R.H. Boyd, Glass transition temperatures of polymers from molecular dynamics simulations, Macromolecules 27 (1994) 7781–7784.
[21] O. Sindt, J. Perez, J.F. Gerard, Molecular architecture mechanical behaviour relationships in epoxy networks, Polymer 37 (1996) 2989–2997.
[22] C.F. Fan, T. Cagin, Z.M. Chen, K.A. Smith, Molecular modeling of polycarbonate. 1. Force field, static structure, and mechanical properties, Macromolecules 27 (1994) 2383–2391.